Stepped-Frequency Processing by Reconstruction of Target Reflectivity Spectrum

Andrew J. Wilkinson, Richard T. Lord and Michael R. Inggs

Abstract— **This paper describes a processing technique for combining stepped-frequency waveforms efficiently to obtain higher range resolution. Essentially this method involves the reconstruction of a wider portion of the target's reflectivity spectrum by combining the individual spectra of the transmitted narrow-bandwidth pulses in the frequency domain. This paper describes the signal processing steps involved, and shows simulation results which validate and illustrate the method.**

Keywords— **Stepped-frequency processing, synthetic range profile, SRP, target reflectivity spectrum.**

I. Introduction

THE use of stepped-frequency waveforms to obtain high range resolution is well documented [8, 10]. An advantage of the stepped-frequency approach for obtaining high range resolution is the reduction of the instantaneous bandwidth and sampling rate requirements of the radar system.

Synthetic range profile (SRP) processing is a very effective method to obtain high-resolution downrange profiles of targets [10]. This method, however, has the unfortunate drawback that target energy spills over into consecutive coarse range bins due to the matched filter operation, causing "ghost images" in the resulting range profile [3]. This is the main reason why it is not regarded as a suitable method for processing SAR images. A time-domain method which does not have this drawback has already been demonstrated [5, 6]. However this method has been found to be inefficient due to the upsampling requirement of the narrow-bandwidth signals.

Instead of recombining the stepped-frequency waveforms in the time-domain, they can also be recombined in the frequency domain. Essentially the aim is to reconstruct a larger portion of the target's reflectivity spectrum by combining the individual spectra of the transmitted narrow-bandwidth pulses in the frequency domain. The target reflectivity function $\varsigma(t)$ represents the target's reflection properties at range r mapped into the time domain, where $t = \frac{2r}{c}$. The principle of enhancing the range resolution by recovering a larger band of the reflectivity's spectrum was introduced by Prati and Rocca [7], but in the context of coherent combination of SAR images taken from different observation angles. In this paper we show how this concept may be applied to the concept of stepped-frequency processing, and describe the signal processing steps involved.

The authors are with the Radar Remote Sensing Group, University of Cape Town, Rondebosch 7701, South Africa. Phone +27 21 650 3756, Fax +27 21 650 3465, Email: rlord@elec-eng.uct.ac.za.

II. Waveform Modelling

A linear FM chirp waveform at baseband can be described by

$$p(t) = A\,\mathrm{rect}\left(\frac{t}{T_p}\right) e^{j\pi\gamma t^2} \tag{1}$$

where A is the amplitude, T_p the pulse length and γ the chirp rate. The spectrum is approximately rectangular with bandwidth $B_{tx} \approx \gamma T_p$. This is a good approximation for linear FM chirp pulses with a high time-bandwidth product.

The transmitted RF signal is modelled by

$$v_{tx}(t) = p(t)\, e^{j2\pi f_c t} \tag{2}$$

where f_c is the centre frequency. The received signal is given by the convolution of the scene reflectivity function $\varsigma(t)$ and the transmitted pulse:

$$\begin{aligned} v_{rx}(t) &= \varsigma(t) \circledast v_{tx}(t) &(3)\\ &= \int \varsigma(t-\tau)\, v_{tx}(\tau)\, d\tau &(4)\end{aligned}$$

After coherent demodulation, the signal at baseband is given by

$$\begin{aligned} v_{bb}(t) &= v_{rx}(t)\, e^{-j2\pi f_c t} &(5)\\ &= \int \varsigma(t-\tau)\, p(\tau)\, e^{j2\pi f_c \tau}\, d\tau\, e^{-j2\pi f_c t} &(6)\\ &= \int \varsigma(t-\tau)\, e^{-j2\pi f_c (t-\tau)}\, p(\tau)\, d\tau &(7)\\ &= \left[\varsigma(t)\, e^{-j2\pi f_c t}\right] \circledast p(t) &(8)\end{aligned}$$

In accordance with the Nyquist criteria, the I and Q channels of this complex signal are each sampled at a sampling rate of $f_s > B_{tx}$. Fourier transforming $v_{bb}(t)$ we obtain

$$V_{bb}(f) = \varsigma\,(f + f_c)\; P(f) \tag{9}$$

Thus, the spectral representation of the received signal can be viewed as a windowed version of the target's reflectivity spectrum $\varsigma\,(f)$, where the position of the window is determined by the centre frequency, and the shape is determined by the spectrum of the transmitted pulse.

Range compression is achieved by convolving the received signal with a linear compression filter $H(f)$, designed as a trade-off between compressing the received signal into a narrow pulse (with desirable low sidelobe properties) and improving the signal to noise ratio. In the frequency domain the range-compression operation is given by

$$\begin{aligned} V(f) &= V_{bb}(f)\, H(f) &(10)\\ &= \varsigma(f + f_c)\, P(f)\, H(f) &(11)\\ &= \varsigma(f + f_c)\, W(f) &(12)\end{aligned}$$

where $W(f) = P(f)\,H(f)$. The time-domain signal is

$$v(t) = \left[\varsigma(t)\, e^{-j2\pi f_c t}\right] \circledast w(t) \tag{13}$$

The phase of $H(f)$ is always chosen to cancel the phase of $P(f)$, thus $\arg(H(f)) = \arg(P^*(f))$. The amplitude of $H(f)$ is chosen according to the desired time-domain impulse response. For example, if we assume that $P(f)$ is strictly bandlimited to B_{tx}, and if $|P(f)\,H(f)| = 1$ across that bandwidth, then

$$V(f) = \varsigma(f + f_c)\ \mathrm{rect}\left(\frac{f}{B_{tx}}\right) \tag{14}$$

This is simply a bandlimited, shifted version of the target's reflectivity spectrum. Inverse transforming, the time-domain waveform is

$$v(t) = \left[\varsigma(t)\, e^{-j2\pi f_c t}\right] \circledast \mathrm{Sa}\left(\pi B_{tx} t\right) \cdot B_{tx} \tag{15}$$

where $\mathrm{Sa}(x) = \frac{\sin(x)}{x}$. Thus the time-domain impulse response is a *sinc* function with a 3 dB resolution of $\delta t = \frac{1}{B_{tx}}$. The sidelobe response can be reduced by introducing an appropriate frequency-domain window function, at the expense of widening the mainlobe.

III. Reconstruction of Target Spectrum

It is now proposed to reconstruct a wider portion of the target's reflectivity spectrum by piecing together several adjacent subportions of the spectrum, each obtained by separate transmission and reception of pulses of bandwidth B_{tx}, but stepped appropriately in frequency by appropriate choice of the carrier frequency. If the frequency step $\Delta f \leq B_{tx}$, the desired reconstruction is possible. Assuming a sequence of n adjacent windows (indexed by $i = 0, \ldots, n-1$), a broad region of the frequency spectrum can be reconstructed, symmetrical about zero, by shifting each spectrum at baseband by an amount

$$\delta f_i = \left(i + \frac{1-n}{2}\right) \Delta f \tag{16}$$

in the positive direction, and adding together the shifted versions.

If we assume a linear superposition of the shifted subspectra, the reconstructed spectrum as shown in Figure 1 is

$$\begin{aligned} V'(f) &= \sum_{i=0}^{n-1} V_i(f - \delta f_i) && (17)\\ &= \sum_{i=0}^{n-1} \varsigma(f + f_i - \delta f_i)\, W(f - \delta f_i) && (18) \end{aligned}$$

where f_i is the carrier frequency of pulse i and $V_i(f)$ is the frequency spectrum at baseband of pulse i. The shift $(f_i - \delta f_i)$ can, by substitution and simplification, be seen to be the centre frequency f_c' of the entire reconstructed spectrum:

$$\begin{aligned} f_c' &= f_i - \delta f_i && (19)\\ &= (f_0 + i\,\Delta f) - \left(i + \frac{1-n}{2}\right) \Delta f && (20)\\ &= f_0 + \left(\frac{n-1}{2}\right) \Delta f && (21)\\ &= \frac{f_0 + f_{n-1}}{2} && (22) \end{aligned}$$

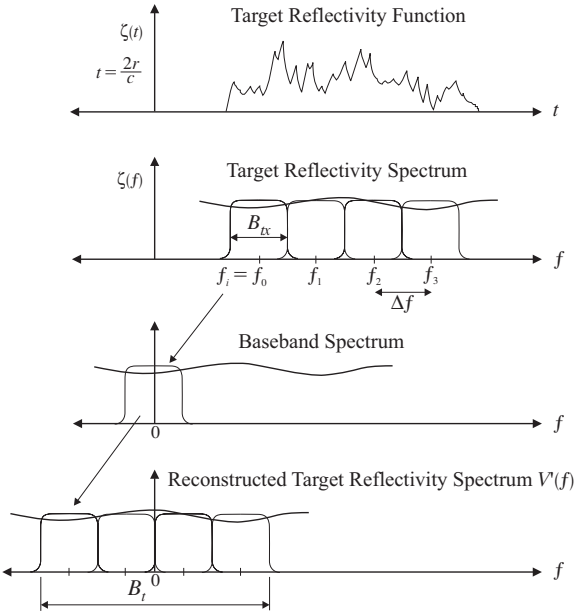

Fig. 1. Reconstruction of the target reflectivity spectrum for $n = 4$ transmitted pulses, each with carrier frequency f_i and bandwidth B_{tx}.

The reconstructed spectrum can thus be expressed as

$$\begin{aligned} V'(f) &= \varsigma(f + f_c') \sum_{i=0}^{n-1} W(f - \delta f_i) && (23)\\ &= \varsigma(f + f_c')\, W'(f) && (24) \end{aligned}$$

where

$$W'(f) = \sum_{i=0}^{n-1} W\left(f - \delta f_i\right) \tag{25}$$

The time-domain signal can then be obtained by inverse transforming to yield

$$v'(t) = \varsigma(t)\, e^{-j2\pi f_c' t} \circledast w'(t) \tag{26}$$

If, for example, we consider the case where the frequency step $\Delta f = B_{tx}$, then the total bandwidth of the reconstructed spectrum is $B_t = nB_{tx}$, as is shown in Figure 1. If the combined compression filter

$$H'(f) = \sum_{i=0}^{n-1} H(f - \delta f_i) \tag{27}$$

is chosen such that $W'(f) = \mathrm{rect}\left(\frac{f}{B_t}\right)$, then the time-domain signal is

$$v'(t) = \varsigma(t)\, e^{-j2\pi f_c' t} \circledast \mathrm{Sa}(\pi B_t t) \cdot B_t \tag{28}$$

and the 3 dB resolution is $\delta t' = \frac{1}{B_t}$, which is a factor of n better than would have been achieved without reconstruction.

Table I: Simulation Parameters

first centre frequency	f_0	5.2625 GHz
frequency step size	Δf	25 MHz
number of steps	n	4
total radar bandwidth	B_t	105 MHz
pulse length	T_p	5 μs
chirp bandwidth	B	30 MHz
ADC (complex) sample rate	f_{ad}	32 MHz

IV. Practical Implementation on Sampled Data

The steps below describe how the spectral reconstruction can be performed with sampled data.

1. Choose a range of carrier frequencies $f_0, \ldots, f_{n-1}$ spaced at Δf equal to, or marginally less than B_{tx}. If $\Delta f > B_{tx}$, the reconstructed spectrum will contain gaps and the resulting time-domain range profile will possess undesirable properties in the form of repeated artifacts spaced at multiples of $\frac{1}{\Delta f}$. However even if there are gaps, an improvement in mainlobe resolution is still possible.
2. For each pulse obtain a sampled version of $v_{bb}(t)$, starting at t_0, with $f_s > B_{tx}$ being the complex sample rate.
3. Apply an FFT to each sampled pulse to obtain the individual subspectra of the target's reflectivity spectrum.
4. To obtain an optimal SNR, it is important to sum the signals with appropriate weighting in the overlap regions. This may be realised by matched-filtering each subspectra prior to addition.
5. Since $v_{bb}(t)$ was sampled starting at t_0, each subspectrum has to be multiplied by the delay compensation factor $\exp(+j2\pi f t_0)$.
6. Shift the spectrum of pulse i to its appropriate location, centred on $f = \left(i + \frac{1-n}{2}\right)\Delta f$.
7. Form the combined spectrum by coherently adding the individual subspectra (see Figure 2).
8. Multiply the combined spectrum by the compression filter $H'(f)$ (see Figure 3) to obtain the discrete equivalent of $V'(f)$ (see Figure 4).
9. Multiply the entire spectrum with $\exp(-j2\pi f t_0)$. This re-shifts the time domain back to a sampled set beginning at $t = t_0$.
10. Apply a reshaping window to tailor the time domain response (see Figure 4). This could be a standard Hanning or Taylor window.
11. Inverse FFT the entire spectrum to obtain the high-resolution range profile (see Figure 5).

V. Design of Compression Filter

The design of the compression filter $H'(f)$ is the most critical and important step in this method. It is important to consider the following points when constructing this filter:

- Obtain an estimate of the impulse response spectrum $P'(f) = \sum_{i=0}^{n-1} P(f - \delta f_i)$. Ideally, for a real system, this should be achieved by measuring the return of a real, physical point target, for example a corner reflector, and recombining the individual spectra as described in the previous section. For such a target $\varsigma(f) \approx \alpha$, where α is a constant, and therefore the combined baseband spectrum would be $V'_{bb}(f) \approx \alpha P'(f)$. This method automatically includes receiver distortions.
- If it is impractical or impossible to obtain the return of a real, physical point target, a point target simulation may be used. It might be difficult, however, to predict receiver distortions. Note that the position of the high-resolution profile will be relative to the target range chosen in the simulation and may therefore need to be shifted.
- If the sampled data has already been range-compressed by a matched filter to optimise SNR, the subspectra used in constructing $H'(f)$ must also be range-compressed first.
- When using a simulation it is important to ensure that there is no aliasing and that the individual subspectra are bandlimited.
- Having obtained an approximation of $P'(f)$, the filter $H'(f)$ is piecewise defined as follows:

$$H'(f) = \begin{cases} \frac{P'^*(f)}{|P'(f_a)|} & \text{for} \quad f \le f_a \\ \frac{1}{P'(f)} & \text{for} \quad f_a < f < f_b \\ \frac{P'^*(f)}{|P'(f_b)|} & \text{for} \quad f \ge f_b \end{cases} \tag{29}$$

where the region $[f_a, f_b]$ includes the major part of the reconstructed spectrum, containing all

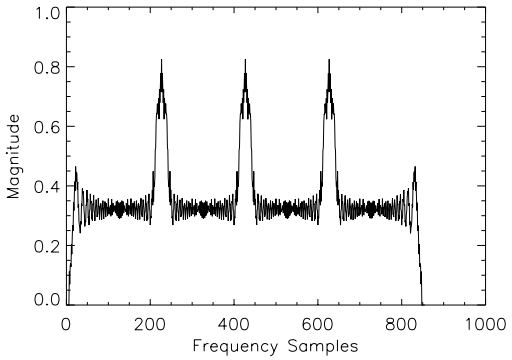

Fig. 2. Spectrum obtained after coherent addition of frequency-shifted subspectra.

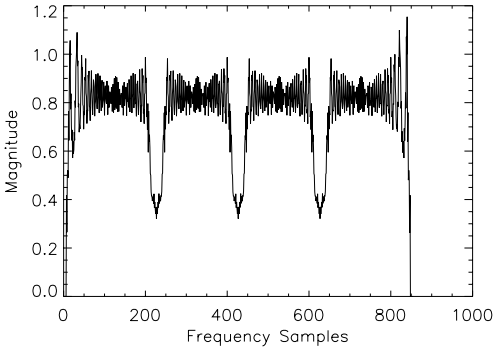

Fig. 3. Spectrum of compression filter $H'(f)$.

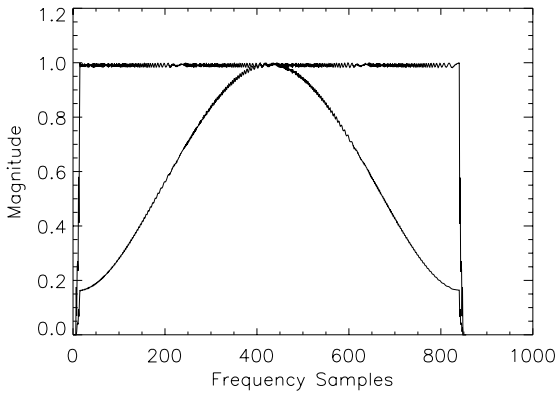

Fig. 4. Target reflectivity spectrum $V'(f)$ after applying compression filter, and after applying reshaping window.

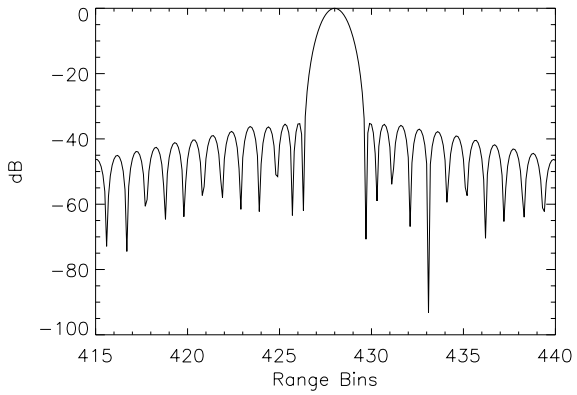

Fig. 5. Section of high-resolution range profile showing point target.

the subspectra boundaries. This will effectively smoothen any ripples at the subspectra boundaries, yielding the desired time-domain impulse response. The first section and the last section of $H'(f)$, where the target spectrum decays to zero, is equated to the conjugate of $P'(f)$. This prevents the amplification of noise for a real system, while still cancelling the phase correctly. Note that $P'(f)$ has to be scaled appropriately so that no discontinuities arise at $H'(f_a)$ and $H'(f_b)$.

VI. Simulation Results

A stepped-frequency radar system was simulated to validate and illustrate the method described above. Table I summarises the relevant parameters used. Four transmitter pulses were simulated, each with a bandwidth of 30 MHz, spaced at 25 MHz intervals, with an overlap of 5 MHz between adjacent subspectra. The total radar bandwidth is 105 MHz.

Figure 2 shows the magnitude of the reconstructed target reflectivity spectrum. The "ripples" at the three subspectra boundaries are clearly visible. After applying the compression filter shown in Figure 3 one obtains the spectrum shown in Figure 4, which closely approximates the desired rect function. A window function has been applied to this spectrum to reduce sidelobe levels. Inverse Fourier transforming this spectrum yields the time-domain high-resolution profile. A dB-plot of a section of this profile is shown in Figure 5, with sidelobe levels at approximately −35 dB.

VII. Conclusions

The method described in this paper efficiently uses all the information obtained from the stepped-frequency waveforms to produce a high-resolution range profile of the illuminated target scene. The execution of the signal processing steps is fast compared to time-domain implementations, since only FFTs and phase multiplications are required, and no upsampling of the narrow-bandwidth pulses is necessary. Furthermore this method is extremely flexible in the sense that the individual pulses may have different bandwidths, the frequency spacing between pulses may vary, the subspectra may (should) overlap in the frequency domain and the individual frequency steps may already be range-compressed. The resulting range profile does not suffer from multiple "ghost" images, except if the construction of the compression filter $H'(f)$ is such that the reconstructed target spectrum contains ripples at the subspectra boundaries. It is therefore important that great care is invested in the design of the compression filter.

Acknowledgments

The authors wish to thank Rolf Lengenfelder, whose radar simulator was used to create the simulated data, and Jasper Horrell for his suggestions and advice.

References

[1] A. Gustavsson, P.O. Frölind, H. Hellsten, T. Jonsson, B. Larsson and G. Stenström, "The Airborne VHF SAR System CARABAS," *Proc. IEEE Geoscience Remote Sensing Symp.*, IGARSS'93, Tokyo, Japan, vol. 2, pp. 558–562, August 1993.

[2] Y. Huang, Z. Ma and S. Mao, "Stepped-frequency SAR System Design and Signal Processing," *Proc. European Conference on Synthetic Aperture Radar*, EUSAR'96, Königswinter, Germany, pp. 565–568, March 1996.

[3] M.R. Inggs, M.W. van Zyl and A. Knight, "A Simulation of Synthetic Range Profile Radar," *Proc. IEEE South African Symp. on Communications and Signal Processing*, COMSIG'92, Cape Town, South Africa, pp. 1–6, September 1992.

[4] R.T. Lord and M.R. Inggs, "High Resolution VHF SAR Processing Using Synthetic Range Profiling," *Proc. IEEE Geoscience Remote Sensing Symp.*, IGARSS'96, Lincoln, Nebraska, vol. 1, pp. 454–456, June 1996.

[5] R.T. Lord and M.R. Inggs, "High Resolution SAR Processing Using Stepped-Frequencies," *Proc. IEEE Geoscience Remote Sensing Symp.*, IGARSS'97, Singapore, vol. 1, pp. 490–492, August 1997.

[6] R.T. Lord and M.R. Inggs, "High Range Resolution Radar using Narrowband Linear Chirps offset in Frequency," *Proc. IEEE South African Symp. on Communications and Signal Processing*, COMSIG'97, Grahamstown, South Africa, pp. 9–12, September 1997.

[7] C. Prati and F. Rocca, "Range Resolution Enhancement with Multiple SAR Surveys Combination," *IEEE*, 1992.

[8] J.A. Scheer and J.L. Kurtz, *Coherent Radar Performance Estimation*, Norwood, MA 02062: Artech House, 1993.

[9] L.M.H. Ulander and H. Hellsten, "System Analysis of Ultra-Wideband VHF SAR," RADAR'97, Edinburgh, UK, Included in conference publication no. 449, pp. 104–108, *IEE*, London, October 1997.

[10] D.R. Wehner, *High-Resolution Radar*, Second Edition, Norwood, MA 02062: Artech House, 1995.